

Nodes in the Order Parameter of Superconducting Iron Pnictides Observed by Infrared Spectroscopy

D. Wu,¹ N. Barišić,¹ M. Dressel,¹ G. H. Cao,² Z. A. Xu,² J. P. Carbotte,³ and E. Schachinger⁴

¹*Physikalisches Institut, Universität Stuttgart,
Pfaffenwaldring 57, 70550 Stuttgart, Germany*

²*Department of Physics, Zhejiang University,
Hangzhou 310027, People's Republic of China*

³*Department of Physics and Astronomy,
McMaster University, Hamilton, Ontario L8S 4M1, Canada*

⁴*Institut für Theoretische Physik, Technische Universität Graz,
Petersgasse 16, 8010 Graz, Austria*

(Dated: November 7, 2018)

Abstract

The temperature and frequency dependences of the conductivity are derived from optical reflection and transmission measurements of electron doped BaFe₂As₂ crystals and films. The data is consistent with gap nodes or possibly a very small gap in the crossover region between these two possibilities. This can arise when one of the several pockets known to exist in these systems has extended *s*-wave gap symmetry with an anisotropic piece canceling or nearly so the isotropic part in some momentum direction. Alternatively, a node can be lifted by impurity scattering which reduces anisotropy. We find that the smaller gap on the hole pocket at the Γ point in the Brillouin zone is isotropic *s*-wave while the electron pocket at the M point has a larger gap which is anisotropic and falls in the crossover region.

PACS numbers: 74.25.Gz, 74.70.Xa 74.20.Rp 74.20.Mn

It took almost ten years from the discovery of high-temperature superconductivity in cuprates to the confirmation of d -wave symmetry of the order parameter and its general acceptance. While only phase sensitive tunneling experiments could prove the change in sign of the wave function [1], previous experiments on the electrodynamic properties provided compelling evidence for nodes in the gap [2]. When the new iron-based superconductors were discovered in 2008 [3], the momentum dependence of the gap function $\Delta(\mathbf{k})$ was raised as one of the most important questions of fundamental relevance [4, 5]. The magnitude of the gap and the quantum mechanical phase of the electron pairs in \mathbf{k} space provides information needed to identify the pairing mechanism. Compared to cuprates, the situation here is more complicated since five bands are close to this Fermi level from which two are most relevant for the physical behavior [6, 7].

Various experimental methods have been applied to elucidate the gap structure of iron pnictides (for recent reviews, see Refs. [5, 8, 9]); however, the results are often contradictory even within the doped BaFe_2As_2 compounds of the 122 family: Specific heat [10, 11], heat transport measurements [12, 13], the temperature dependence of the penetration depth [14–16], tunneling spectroscopy (STM) [17, 18], spin-lattice relaxation [19–21], muon spin rotation (μSR) [22–24] and electronic Raman scattering [25] are discussed controversially, since the results might depend on the sample quality, doping regime or particular system. Angle-resolved photoemission spectroscopy (ARPES) consistently detects nodeless, isotropic superconducting gaps on all sheets of the Fermi surface [26, 27] but might be hampered by resolution problems. According to their interpretation, gaps open simultaneously below T_c with two distinct energies on different parts of the Fermi surface: approximately 5 meV (Γ point) and 12 meV (Γ point and M point). There is also a second pocket centered at Γ with a smaller radius and a gap of 12 meV but often this is not included in the simplest two pocket model as we will employ here. This is taken as evidence for an s -wave pairing state [5, 7] but remains silent as to whether or not the state is of s^\pm -type, i.e., the symmetry of the order parameter reverses sign for electron and hole pockets on the Fermi surface. On the other hand new phase sensitive scanning tunneling microscopy (STM) data [28] have provided strong evidence for s^\pm symmetry which we will assume to be the case in this paper.

Optical experiments might contribute to clarify these issues for the superconducting con-

densate and electronic excitations can be probed with very high resolution over a wide energy range. Hence, microwave, THz and infrared methods have been the primary tool to investigate the energy gap of conventional superconductors [29, 30], and have been applied to iron pnictides, in particular to 122 compounds by single crystal reflection [31–37] and films transmission [38–40] experiments.

We have measured the optical reflectivity of $\text{Ba}(\text{Fe}_{0.92}\text{Co}_{0.08})_2\text{As}_2$ and $\text{Ba}(\text{Fe}_{0.95}\text{Ni}_{0.05})_2\text{As}_2$ single crystals ($T_c = 25$ and 20 K) off the ab surface over a wide frequency and temperature range [34, 41]. The complex conductivity $\hat{\sigma} = \sigma_1 + i\sigma_2$ is calculated via Kramers-Kronig analysis and further analyzed by the extended Drude model [30] in order to obtain the frequency dependent optical scattering rate $\tau^{-1}(\omega)$ related to the total optical conductivity by $\tau^{-1}(\omega) = \omega_p^2 \text{Re}\{\hat{\sigma}^{-1}(\omega)\}/(4\pi)$ with ω_p the plasma frequency.

In Fig. 1(a) the change in the optical reflectivity of $\text{Ba}(\text{Fe}_{0.92}\text{Co}_{0.08})_2\text{As}_2$ is plotted for different temperatures below $T_c = 25$ K. The maximum in $R(\omega, T)/R(\omega, T = 30 \text{ K})$ at approximately 5 meV is a clear indication that a superconducting gap of this energy opens. However, looking at the corresponding conductivity plotted in panel (b), it becomes obvious that $\sigma_1(\omega, T)/\sigma_1(\omega, T = 30 \text{ K})$ does not drop to zero at the gap as rapidly as expected for a simple s -wave superconductor [29, 30], but decreases in an almost linear fashion before it increases again at very low energies. This is the hallmark of nodes in the gap for which excitations are possible at infinitely small energies. The corresponding optical scattering rate is plotted Fig. 1(c).

In order to simultaneously describe these optical properties we decompose the conductivity in two contributions $\hat{\sigma} = \hat{\sigma}^{(1)} + \hat{\sigma}^{(2)}$, corresponding to a hole band [$\omega_p^{(1)}/(2\pi c) \approx 0.58 \text{ eV}$] and an electron band [$\omega_p^{(2)}/(2\pi c) \approx 1 \text{ eV}$]. In order to keep the number of fit parameters minimal we have chosen a single scattering rate for both terms [42]. The superconducting state is mimicked by a two-gap BCS model with an isotropic s -wave gap $2\Delta_0^{(1)} = 5 \text{ meV}$ on the hole pocket, while the gap on the electron pocket was modeled with an extended s -wave gap which when referred to the M point as origin takes on the form $\Delta^{(2)} = \Delta_s + \Delta_d \sqrt{2} \cos\{2\theta\}$ (Δ_s is the s -wave component, Δ_d is the amplitude of the d -wave component, and θ is the polar angle on the Fermi surface). Here $\Delta_s = \alpha \Delta_0^{(2)}$ and $\Delta_d = \sqrt{1 - \alpha^2} \Delta_0^{(2)}$, where $\Delta_0^{(2)} = \sqrt{\langle [\Delta^{(2)}(\theta)]^2 \rangle_\theta}$, $\langle \dots \rangle_\theta$ the Fermi-surface average and $2\Delta_0^{(2)} = 15 \text{ meV}$. The percent-

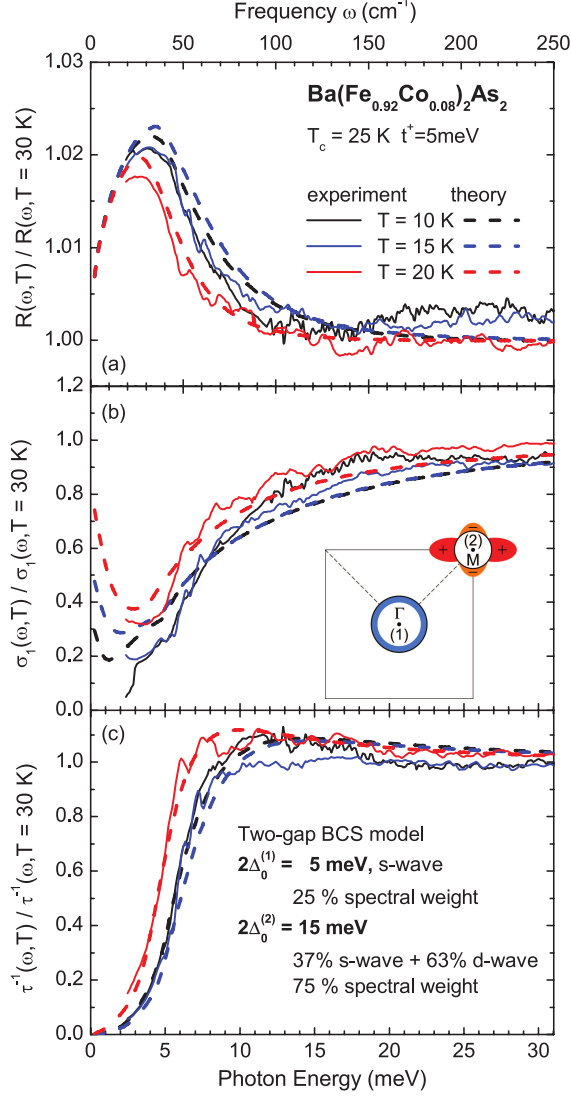


FIG. 1: (Color online) Relative change of the optical properties of $\text{Ba}(\text{Fe}_{0.92}\text{Co}_{0.08})_2\text{As}_2$ upon entering the superconducting state at $T_c = 25$ K. The solid lines correspond to experimental data obtained at $T = 10, 15$ and 30 K. The dashed lines represent fits by a two gap model with different symmetry, where the first gap $2\Delta_0^{(1)} = 5$ meV has a simple s -wave symmetry, while the second gap exhibits $s + d$ wave symmetry with 37% s -wave character and an amplitude $2\Delta_0^{(2)} = 15$ meV. (a) Reflectivity $R(\omega, T)/R(\omega, T = 30 \text{ K})$, (b) optical conductivity $\sigma_1(\omega, T)/\sigma_1(\omega, T = 30 \text{ K})$, and (c) frequency dependent optical scattering rate $\tau^{-1}(\omega, T)/\tau^{-1}(\omega, T = 30 \text{ K})$. The inset sketches the two Fermi-surface pockets in \mathbf{k} space, with an isotropic s -wave gap about Γ and an anisotropic extended s -wave gap about M .

age of s -wave component is expressed by $x = \alpha/(\alpha + \sqrt{1 - \alpha^2})$ [43]. We refer to this model as extended s^\pm .

As seen from Fig. 1, the fit to the experimental data and derived quantities is remarkably good; even small details and particular features are described well, such as the increase in $R(\omega, T)/R(\omega, 30 \text{ K})$ as the temperature is lowered, the shift of the peak to higher frequencies, the gradual drop in $\sigma_1(\omega, T)/\sigma_1(\omega, 30 \text{ K})$ without approaching zero, but showing an upturn as $\omega \rightarrow 0$, the slight increase of the scattering rate as ω decreases with a rapid drop when the smaller gap is reached, but also the way it approaches zero. The consistent description of all quantities in the complete frequency and temperature range with a single set of parameters gives confidence in the proper choice of the model. In all calculations the temperature dependence of the superconducting gaps was modeled by the BCS mean field dependence.

The comparison with optical data obtained by transmission experiments of thin films of Co doped BaFe_2As_2 [39, 40] corroborates our hypothesis. The pronounced coherence peak observed in the microwave conductivity $\sigma_1(T)$ below T_c is significantly broader than expected from simple s -wave BCS theory [29, 30] and extends to much lower temperatures; but it can be perfectly reproduced by the present model with basically the same set of parameters [44]. This also includes the quadratic temperature dependence of the penetration depth $\lambda \propto T^2$ at the lowest temperatures (see also Modre *et al.* [45]).

To better understand our results it is important to consider very low temperatures considerably below the lowest experimental temperature given in Fig. 1. In Fig. 2 we show results for an extended s -wave gap with the same parameters as we have used in our experimental fit [42] with the reduced temperature set at $t = T/T_c = 0.05$, i.e. $T = 1.25 \text{ K}$. Fig. 2(a) shows $\sigma_1(\omega)$ in meV vs ω also in meV. The various curves are for six different values of the variable x which multiplied by hundred gives the percentage of the s -wave component in an $s + d$ -wave admixture as labeled. The case $x = 0.37$ corresponds to the anisotropy we used in our fit to experiment. We see that this corresponds to a very small but finite spectral gap in the real part of the optical conductivity. This gap is so small, however, that it falls near the end of the available THz range and is not present at 10 K where we have a gapless behavior. In Fig. 2(b) we show the same results but normalized to the real part of the optical conductivity $\sigma_1(\omega, T = 30 \text{ K})$ at $T = 30 \text{ K}$ in the normal state while in Fig. 2(c) we show

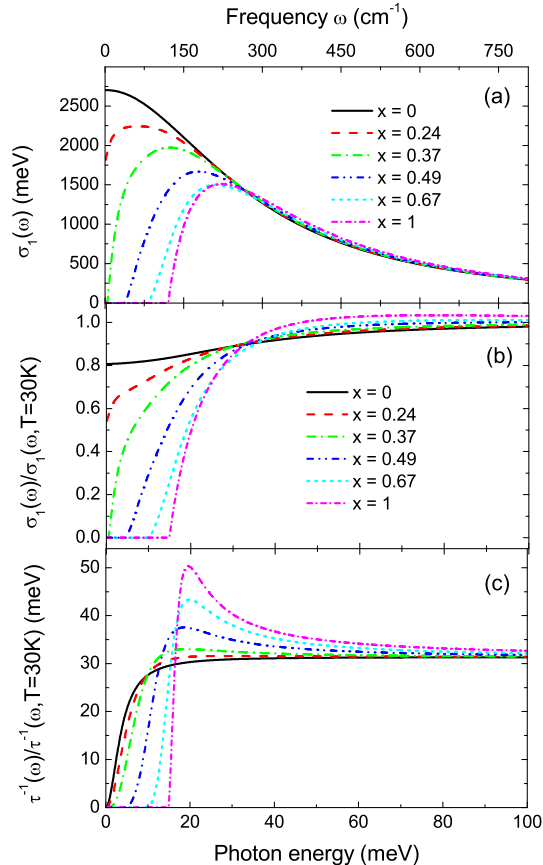


FIG. 2: (Color online) (a) The real part of the optical conductivity $\sigma_1(\omega)$ in meV vs the photon energy ω in meV for an $s + d$ -wave model at $T = 1.25$ K and for various values of the parameter x which multiplied by hundred gives the percentage of the s -wave admixture. Thus, $x = 0$ corresponds to pure d -wave symmetry of the gap while $x = 1$ corresponds to s -wave symmetry. $\Delta_0 = 7.5$ meV and the elastic scattering rate $\tau_{\text{imp}}^{-1} = 31.4$ meV. The $x = 0.37$ corresponds to the s -wave admixture used in the analysis presented in Fig. 1. (b) The same as (a) but for the normalized real part of the optical conductivity $\sigma_1(\omega)/\sigma_1(\omega, T = 30 \text{ K})$ with $\sigma_1(\omega, T = 30 \text{ K})$ its normal state value. (c) The same as (a) but for the normalized optical scattering rate $\tau^{-1}(\omega)/\tau^{-1}(\omega, T = 30 \text{ K})$. It is clear from these results that it would be very difficult even at low temperatures to differentiate between nodes and the case of a small spectral gap. All we can firmly conclude from our present analysis is that the material studied falls close to the crossover region between these two possibilities.

In order to proof the general applicability of our description, we have analyzed the optical

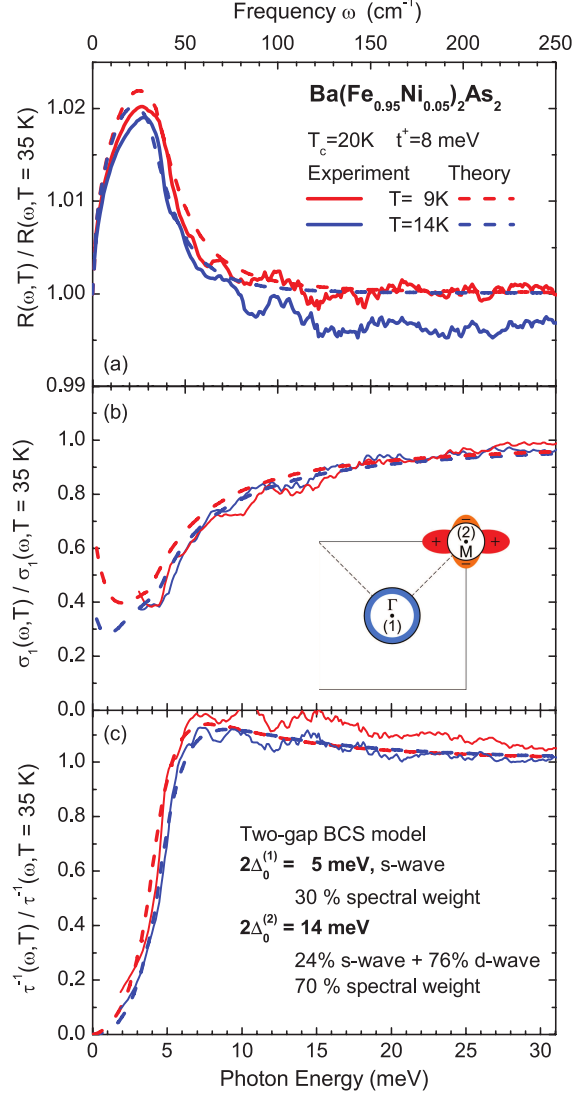


FIG. 3: (Color online) Relative change of the optical properties of $\text{Ba}(\text{Fe}_{0.95}\text{Ni}_{0.05})_2\text{As}_2$ upon entering the superconducting state at $T_c = 20\text{ K}$. The solid lines correspond to experimental data obtained at $T = 9$ and 14 K . The dashed lines represent fits by a two gap model with different symmetry, where the first gap $2\Delta_0^{(1)} = 4.5\text{ meV}$ has a simple s -wave symmetry, while the second gap exhibits $s + d$ wave symmetry with 24% s -wave character and an amplitude $2\Delta_0^{(2)} = 14\text{ meV}$. (a) Reflectivity $R(\omega, T)/R(\omega, T = 35\text{ K})$, (b) optical conductivity $\sigma_1(\omega, T)/\sigma_1(\omega, T = 35\text{ K})$, and (c) frequency dependent optical scattering rate $\tau^{-1}(\omega, T)/\tau^{-1}(\omega, T = 35\text{ K})$.

data for $\text{Ba}(\text{Fe}_{0.95}\text{Ni}_{0.05})_2\text{As}_2$ in a similar fashion. Fig. 3 displays the corresponding results for $T = 9$ and 14 K, referenced to the normal state data measured at $T = 35$ K. In this case the extended s^\pm model is defined by the isotropic s -wave gap of $2\Delta_0^{(1)} = 4.5$ meV for 30% of the spectral weight, while the dominant electron band is gapped of size $2\Delta_0^{(2)} = 14$ meV with $x = 0.24$ and contains nodes. The distribution of spectral weight between both gaps is $w = w^{(1)} + w^{(2)} = 0.3 + 0.7$. The plasma frequency was set to $\omega_p = 1.3$ eV and the elastic scattering rate to $\tau_{\text{imp}}^{-1} = 50$ meV. Again, the agreement between experiment and theory is very good, considering that the lower energy scale approaches the limit of the frequency range accessible by experiment.

In conclusion, we have analyzed the temperature and frequency dependences of the optical properties of electron doped BaFe_2As_2 in the superconducting state. From the low-frequency reflectivity and conductivity ratios R_s/R_n and σ_s/σ_n below and above T_c , we conclude the symmetry of the order parameter can be described by an extended s^\pm model. Two gaps are needed to get agreement. The smaller gap is isotropic s -wave while the larger gap is anisotropic with nodes, or possibly with a very small spectral gap. When referred to the M point in the Brillouin zone as origin it is described as a mixture of s and d -wave with the d -wave component providing a mechanism for gap nodes or a very small gap in certain directions in momentum space. This is strongly supported by a broad coherence peak in the microwave conductivity $\sigma_1(T)$ and the temperature dependence of the penetration depth $\lambda(T) \propto T^2$ observed in optical transmission measurements through films. Our theoretical two gap model gives $\lambda(T) \propto T^{1.9}$ which is in very good agreement with experiment. Finally, we note that optics cannot distinguish between gap phases (it is not phase sensitive) but recent STM experiments [28] firmly established the s^\pm symmetry with electron and hole pockets having the opposite sign.

We appreciate discussions with D.N. Basov, N. Drichko, C. Haule, D. van der Marel and A.V. Pronin. N.B. and D.W. acknowledge a fellowship of the Alexander von Humboldt-Foundation. G. H. Cao and Z-A. Xu acknowledge partial support from NSFC.

-
- [1] D. J. Van Harlingen, Rev. Mod. Phys. **67**, 515 (1995); C. C. Tsuei and J. R. Kirtley, Rev. Mod. Phys. **72**, 969 (2000).
- [2] W. N. Hardy, D. A. Bonn, D. C. Morgan, R. Liang, and K. Zhang, Phys. Rev. Lett. **70**, 3999 (1993).
- [3] Y. Kamihara, T. Watanabe, M. Hirano, and H. Hosono, J. Am. Chem. Soc. **130**, 3296 (2008).
- [4] S.A. Kivelson and H. Yao, Nature Materials **7**, 927 (2008).
- [5] I.I. Mazin, Nature **464**, 183 (2010).
- [6] J. Fink *et al.*, Phys. Rev. B **79**, 155118 (2009).
- [7] I. I. Mazin, D. J. Singh, M. D. Johannes, and M. H. Du, Phys. Rev. Lett. **101**, 057003 (2008); I. I. Mazin and J. Schmalian, Physica C **469**, 614 (2009).
- [8] K. Ishida, Y. Nakai, and H. Hosono, J. Phys. Soc. Jpn. **78**, 062001 (2009).
- [9] D.C. Johnston, arXiv:1005.4392 (*unpublished*) (2010).
- [10] K. Gofryk *et al.*, New J. Phys. **12**, 023006 (2010).
- [11] G. Mu *et al.*, Chin. Phys. Lett. **27**, 037402 (2010).
- [12] J. K. Dong *et al.*, Phys. Rev. B **81**, 094520 (2010)
- [13] X. G. Luo *et al.*, Phys. Rev. B **80**, 140503 (2009); M. A. Tanatar *et al.*, Phys. Rev. Lett. **104**, 067002 (2010); J.-P. Reid *et al.*, arXiv:1004.3804.
- [14] K. Hashimoto *et al.*, Phys. Rev. Lett. **102**, 207001 (2009).
- [15] R. T. Gordon *et al.*, Phys. Rev. Lett. **102**, 127004 (2009); C. Martin *et al.*, Phys. Rev. B **80**, 020501 (2009); C. Martin *et al.*, Phys. Rev. B **81**, 060505 (2010).
- [16] V. Mishra *et al.*, Phys. Rev. B **79**, 094512 (2009).
- [17] P. Szabó *et al.*, Phys. Rev. B **79**, 012503 (2009); D. Wang, Y. Wan, and Q.-H. Wang, Phys. Rev. Lett. **102**, 197004 (2009).
- [18] P. Samuely *et al.*, Physica C **469**, 507 (2009).
- [19] H. Fukazawa *et al.*, J. Phys. Soc. Jpn. **78**, 033704 (2009).
- [20] Y. Nakai *et al.*, Phys. Rev. B **81**, 020503 (2010).
- [21] S. W. Zhang *et al.*, Phys. Rev. B **81**, 012503 (2010).

- [22] M. Hiraishi *et al.*, J. Phys. Soc. Jpn. **78**, 023710 (2009).
- [23] T. Goko *et al.*, Phys. Rev. B **80** 024508 (2009).
- [24] R. Khasanov *et al.*, Phys. Rev. Lett. **102**, 187005 (2009).
- [25] B. Muschler *et al.*, Phys. Rev. B **80**, 180510 (2009).
- [26] K. Terashima *et al.*, Proc. Nat. Acad. Sci. (New York) **106**, 7330 (2009); K. Nakayama *et al.*, Europhys. Lett. **85**, 67002 (2009); H. Ding *et al.*, EPL **83**, 47001 (2008).
- [27] D. V. Evtushinsky *et al.*, New J. Phys. **11**, 055069 (2009); D. V. Evtushinsky *et al.*, Phys. Rev. B **79**, 054517 (2009).
- [28] T. Hanaguri, S. Niitaka, K. Kuroki, and H. Takagi, Science **328**, 474 (2010).
- [29] M. Tinkham, *Introduction to Superconductivity*, 2nd edition (McGraw-Hill, New York, 1996).
- [30] M. Dressel and G. Grüner, *Electrodynamics of Solids* (Cambridge University Press, Cambridge, 2002).
- [31] G. Li *et al.*, Phys. Rev. Lett. **101** 107004 (2008).
- [32] W. Z. Hu, Q. M. Zhang, and N. L. Wang, Physica C **469** (2009) 545.
- [33] D. Wu *et al.*, Physica C. *in press* arXiv:0912.0849(2009)
- [34] D. Wu *et al.*, Phys. Rev. B **81** 100512(R) (2010).
- [35] K. W. Kim *et al.*, Phys. Rev. B **81**, 214508 (2010).
- [36] E. van Heumen *et al.*, EuroPhys. Lett. **90** 37005 (2010).
- [37] N. Barišić *et al.*, arXiv:1004.1658 (*unpublished*) (2010).
- [38] A. Perucchi *et al.*, EuroPhys. Lett. B *in press* arXiv:1003.0565 (2010).
- [39] B. Gorshunov *et al.*, Phys. Rev. B **81** 060509(R) (2010).
- [40] T. Fischer *et al.*, arXiv:1005.0692 (*unpublished*) (2010).
- [41] We measured the optical conductivity down to 20 cm⁻¹ using IR 1.5K Bolometer. The Hagen-Rubens extrapolation was applied for the low frequency. Below 35 cm⁻¹ we used a proper smoothing procedure to reduce the experimental noise.
- [42] We have chosen $\epsilon_\infty = 10$ to account for higher-energy excitations. The total plasma frequency is $\omega_p/(2\pi c) = 1.15$ eV and the elastic scattering rate $\tau_{\text{imp}}^{-1} = 31.4$ meV. The distribution of spectral weight between both components is $w = w^{(1)} + w^{(2)} = 0.25 + 0.75 = 1$, and $x = 0.37$.
- [43] E. Schachinger and J. P. Carbotte, Phys. Rev. B **80**, 174526 (2009); J.P. Carbotte and E.

Schachinger Phys. Rev. B **81**, 104510 (2010); I. Schürer, E. Schachinger, and J. P. Carbotte, Physica C **303**, 287 (1998).

[44] The energy gaps for the $\text{Ba}(\text{Fe}_{0.9}\text{Co}_{0.1})_2\text{As}_2$ film ($T_c \approx 25$ K) are $2\Delta_0^{(1)} = 6$ meV and $2\Delta_0^{(2)} = 16$ meV. The distribution of spectral weight is the same as found for the crystal: $w^{(1)} = 0.25$ and $w^{(2)} = 0.75$ with $\alpha = 0.45$ corresponding to an s -wave component of $x = 1/3$. See details in Ref.[40]

[45] R. Modre, I. Schürer, and E. Schachinger, Phys. Rev. B **57**, 5496 (1998).